Site-Specific Water Dynamics in the First Hydration Layer of an Anti-Freeze Glyco-Protein: A Simulation Study (Supporting Materials)

Tan Jin[1,2], Fengqin Long[1,2], Qiang Zhang[3*], Wei Zhuang[1,4*]

1. *State Key Laboratory of Structural Chemistry, Fujian Institute of Research on the Structure of Matter, Chinese Academy of Sciences, Fuzhou, Fujian 350002, China*
2. *University of Chinese Academy of Sciences, Beijing 100049, China.*
3. *College of Chemistry and Material Sciences, Inner Mongolia University for Nationalities, Tongliao, Inner Mongolia 028043, China*
4. *Institute of Urban Environment, Chinese Academy of Sciences, Xiamen, Fujian 361021, China*

* To whom correspondence should be addressed. E-mail: wzhuang@fjirsm.ac.cn, qzhang@imun.edu.cn

A. Several Other Schemes for the Rotational Time Constant Calculations.

The rotational time constants were often calculated by fitting the early part (usually 2~10 ps) of the correlation function using a single exponential function $C_{fit}(t)'_{\alpha} = B\exp(-t/\tau'_{\alpha})$ .We also calculated them for methyl and hydroxyl sites in AFGP8 at 300 K with the SPC and HBSEB scheme. In Fig. S2, the SPC retardation factor $\xi'_{\alpha,SPC} = \tau'_{\alpha,SPC} / \tau'_{bulk}$ for methyl and hydroxyl sites are 1.5-3.5 and 1.6-5.2, almost consistent with the previous reported window of 2~5.[1, 2] And the HBSEB retardation factor $\xi'_{\alpha,HBSEB} = \tau'_{\alpha,HBSEB} / \tau'_{bulk}$ for methyl and hydroxyl sites are 1.8-4.5 and 2.4-9.3 respectively, considerably smaller than the integrated time constant $\xi_{\alpha,HBSEB}$ in general. This is because τ'_{α} are calculated by selectively fitting the correlation functions at their early part. Most of the contributions from the slow components, generated from the non-negligible proportion of the fragments longer than 10 ps in $\{f_j\}_{\alpha}^{HBSEB}$ (53% and 32% for the methyl and hydroxyl groups, respectively) are therefore neglected. The contribution from the fast component is dominant. $\xi'_{\alpha,HBSEB}$ are larger than $\xi'_{\alpha,SPC}$ in general but the differences are much smaller than that between $\xi_{\alpha,HBSEB}$ and $\xi_{\alpha,SPC}$.

We also calculated water rotation using a modified SPC scheme, which only takes, for each trajectory in $\{f_j\}_{\alpha}^{SPC}$, the portion from time zero to the moment the target water molecule drifts out of the first hydration layer for the first time. We referred to the related analysis as starting-ending-point-controlled (SEPC). The overall SEPC rotational time constants (Fig. S2) are similar to the HBSEB results and much longer and more inhomogeneous than the SPC results, suggesting the critical role of non-first-layer water motion to the difference between HBSEB and SPC results.

Note the results of SEPC and HBSEB are not exactly the same since the trajectory fragment ensembles they are based on have some differences. These differences may come from the missing fragments that will be away from or enter into the hydration layer during one switch event. So we also carried out the calculation using a HBSEB+ scheme, in which we added these switch events into the fragments of HBSEB. It is obvious that the retardation factors from HBSEB+ are almost the same as SEPC in Fig. S2. This suggests that our selection method does not bias the reorientation dynamic in the hydration layer.

B. Categorization for Water Accessible Surface Sites in AFGP8 and Ubiquitin

The hydrogen bond switch events $\{f_i'\}_\alpha$ were first collected for all first layer water of the whole protein, and classified into different categories according to their locations. For instance, if a switch event happens within the first hydration layer of only a heavy atoms of the backbone but not the disaccharide or the sidechain, we labeled the event as backbone-only, all the events happening within the first layer of the same backbone heavy atom were grouped together for the calculation of water reorientation correlation function of this single site, all these single-site correlation function were then averaged over to calculate the average correlation function for this category. Similarly, we also calculated the averaged single site reorientation correlation functions for other categories.

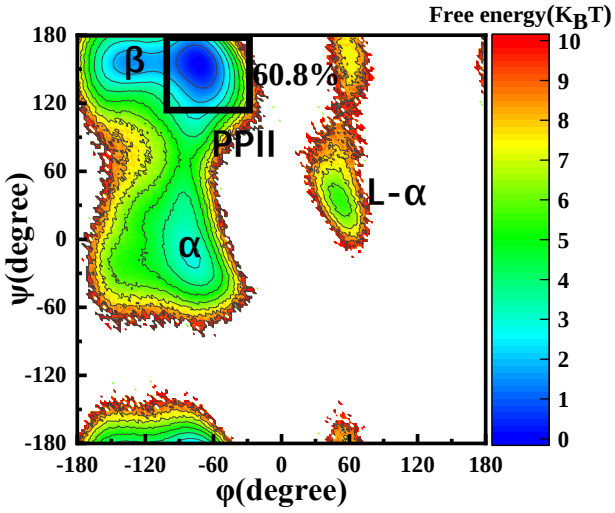

Fig. S1 Ramachandran plot of AFGP8 at 300 K.

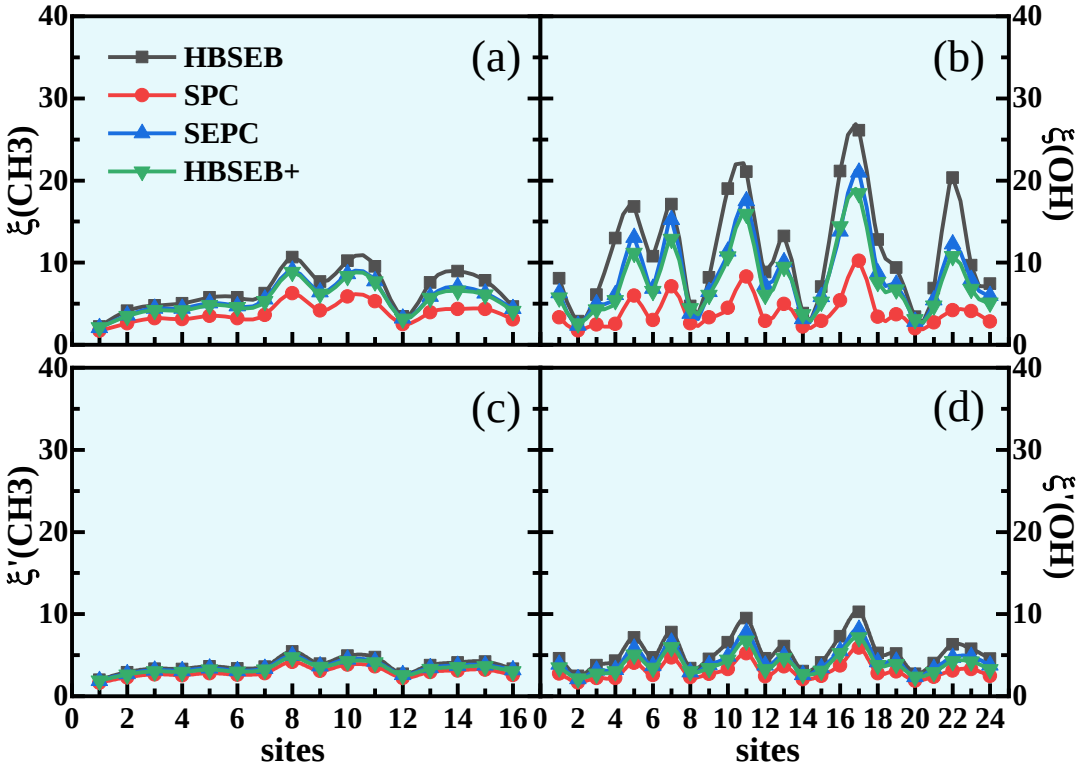

Fig. S2 Overall HBSEB, SPC, SEPC and HBSEB+ hydration water reorientation retardation factors at the methyl (a) and hydroxyl sites (b) at 300 K. HBSEB, SPC, SEPC and HBSEB+ hydration water reorientation retardation factors for methyl sites (c) and hydroxyl sites (d) calculated by fitting the correlation functions within their early part (2-10 ps) using the single exponential function at 300 K.

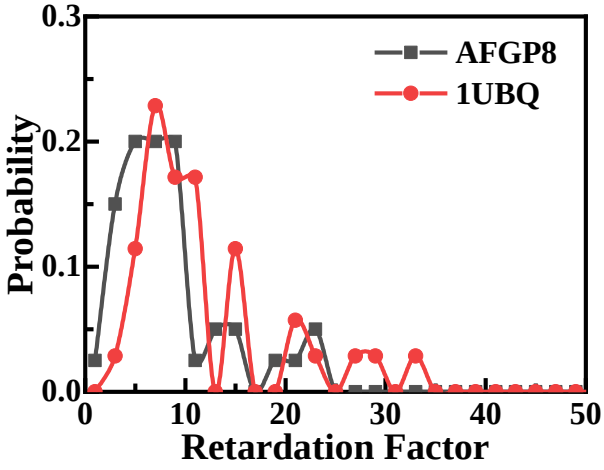

Fig. S3 The distribution of retardation factor between AFGP8 and 1UBQ using HBSEB in the hydration layer for the methyl+hydroxyl groups at 300 K.

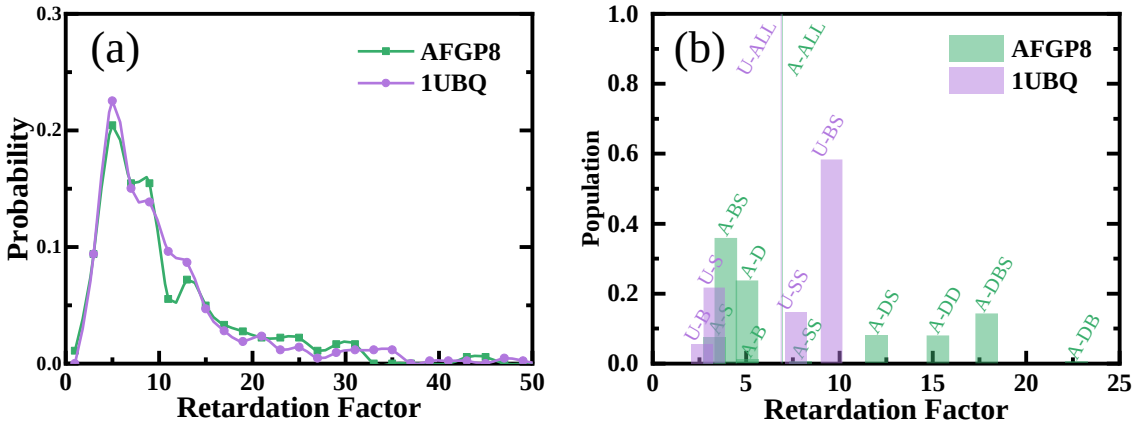

Fig. S4 The probability distribution of HBSEB retardation factor of the first layer water for all the sites in the AFGP8 and ubiquitin at 246 K (a). The populations and rotational retardation factors for different categories of first layer water hydrogen bond switching events on the surface of AFGP8 and ubiquitin at 246 K (b). For AFGP8, the categories include backbone-only (A-B), one-sidechain-only (A-S), one-disaccharide-only (A-D), disaccharide-disaccharide (A-DD), sidechain-sidechain(A-SS), backbone-sidechain (A-BS), disaccharide-backbone (A-DB), disaccharide-sidechain(A-DS), disaccharide-backbone sidechain (A-DBS) and overall (A-ALL). For ubiquitin, the categories include backbone-only(U-B), one-sidechain-only(U-S), sidechain-sidechain(U-SS), backbone-sidechain (U-BS) and overall (U-ALL).

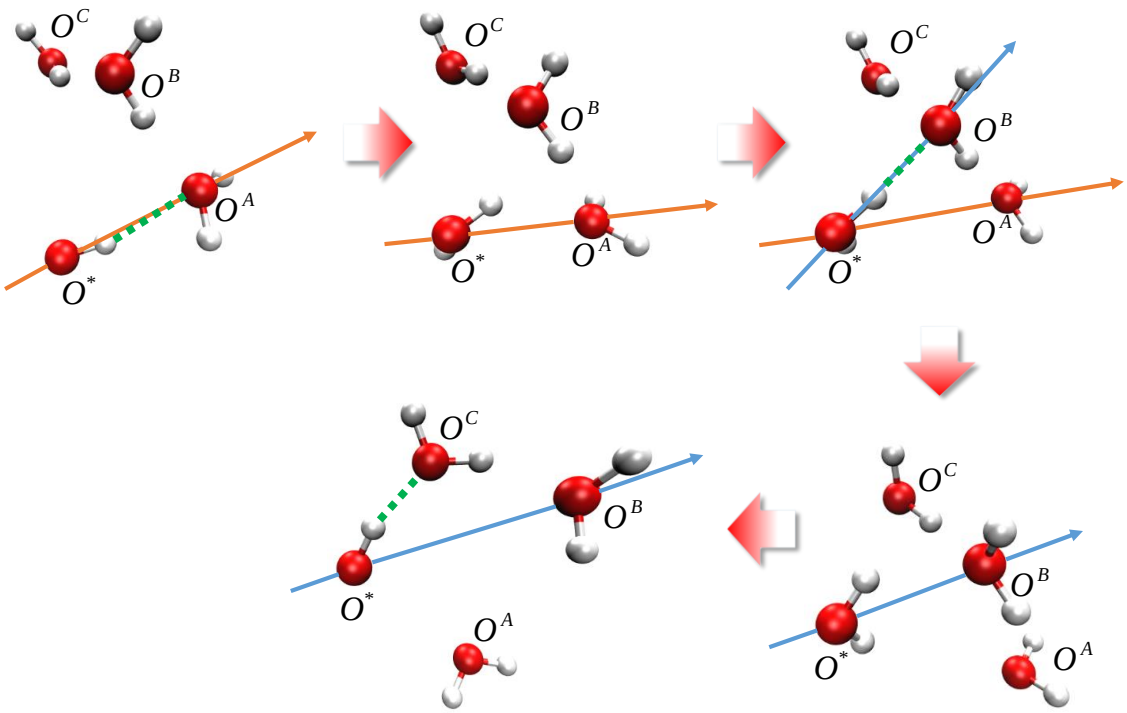

Scheme S1 The cartoon representations of cross-event frame motion. The target water(oxygen atom O^*) jumps from O^A to O^B and then from O^B to O^C including two continue switching events. The molecular frame in the first event is the vector $\overrightarrow{O^*O^A}$ (orange arrow) and the molecular frame in the second event is the vector $\overrightarrow{O^*O^B}$ (blue arrow). To ensure the continuity of cross-event frame correlation function, the frame $\overrightarrow{O^*O^B}$ convers by the rotation matrix which rotate the angle $\angle O^B O^* O^A$ in the joint snapshot between switching events.

Table S1 Tri-exponential fitting parameters and the integrated time (ps) of the HBSEB second rank rotation of hydration layer water molecules around the methyl sites at 300 K.

	A1	τ_1	A2	τ_2	A3	τ_3	$\langle\tau\rangle$	R^2
CH3-1	0.287	0.138	0.500	3.099	0.213	12.143	4.178	0.9996
CH3-2	0.283	0.134	0.487	3.870	0.230	24.665	7.602	0.9994
CH3-3	0.275	0.128	0.439	3.816	0.285	24.027	8.565	0.9995
CH3-4	0.275	0.130	0.448	3.882	0.278	27.667	9.461	0.9994
CH3-5	0.280	0.130	0.463	3.925	0.257	23.754	7.966	0.9995
CH3-6	0.278	0.131	0.452	4.135	0.270	34.792	11.303	0.9993
CH3-7	0.279	0.128	0.440	4.264	0.280	36.800	12.232	0.9993
CH3-8	0.264	0.122	0.385	4.314	0.351	44.031	17.157	0.9994
CH3-9	0.281	0.133	0.464	4.488	0.255	47.556	14.251	0.9992
CH3-10	0.264	0.123	0.398	4.418	0.337	54.139	20.059	0.9992
CH3-11	0.268	0.126	0.408	4.337	0.324	49.878	17.966	0.9993
CH3-12	0.279	0.131	0.470	3.865	0.251	21.584	7.268	0.9995
CH3-13	0.278	0.132	0.464	4.329	0.259	46.835	14.159	0.9993
CH3-14	0.279	0.129	0.452	4.444	0.269	54.496	16.692	0.9992
CH3-15	0.270	0.128	0.421	4.418	0.309	42.837	15.126	0.9993
CH3-16	0.262	0.128	0.424	3.892	0.314	22.460	8.727	0.9996

Table S2 Tri-exponential fitting parameters and the integrated time (ps) of the HBSEB second rank rotation of hydration layer water molecules around the hydroxyl sites at 300 K.

	A1	τ_1	A2	τ_2	A3	τ_3	$\langle\tau\rangle$	R^2

OH-1	0.279	0.121	0.376	3.954	0.346	37.701	14.548	0.9994
OH-2	0.295	0.120	0.415	3.107	0.290	14.288	5.474	0.9996
OH-3	0.288	0.119	0.401	3.603	0.311	33.159	11.802	0.9994
OH-4	0.296	0.122	0.410	3.959	0.294	61.595	19.754	0.9993
OH-5	0.263	0.107	0.293	4.337	0.444	60.103	27.962	0.9993
OH-6	0.292	0.122	0.398	4.569	0.311	74.202	24.911	0.9991
OH-7	0.264	0.113	0.314	4.336	0.422	73.526	32.414	0.9992
OH-8	0.294	0.123	0.421	3.677	0.284	24.839	8.650	0.9995
OH-9	0.284	0.115	0.371	3.647	0.345	37.903	14.479	0.9994
OH-10	0.281	0.112	0.340	3.855	0.379	71.522	28.446	0.9992
OH-11	0.246	0.094	0.231	4.084	0.523	87.374	46.705	0.9992
OH-12	0.292	0.124	0.364	4.206	0.343	45.230	17.102	0.9990
OH-13	0.275	0.117	0.338	3.925	0.387	45.740	19.059	0.9993
OH-14	0.296	0.122	0.428	3.359	0.276	19.691	6.914	0.9994
OH-15	0.291	0.123	0.410	4.001	0.298	50.364	16.707	0.9991
OH-16	0.261	0.095	0.293	3.221	0.445	97.137	44.217	0.9990
OH-17	0.253	0.099	0.257	4.369	0.491	94.324	47.432	0.9991
OH-18	0.287	0.119	0.398	4.846	0.315	93.624	31.474	0.9991
OH-19	0.281	0.119	0.353	3.876	0.365	39.101	15.691	0.9994
OH-20	0.298	0.123	0.437	3.360	0.264	17.711	6.186	0.9995
OH-21	0.286	0.117	0.396	3.635	0.318	34.067	12.316	0.9994
OH-22	0.281	0.114	0.326	4.005	0.393	101.169	41.134	0.9990
OH-23	0.265	0.107	0.305	3.717	0.430	37.585	17.311	0.9995

OH-24	0.296	0.123	0.386	4.136	0.318	52.030	18.190	0.9991

Table S3 Tri-exponential fitting parameters and the integrated time (ps) of the SPC second rank rotation of hydration layer water molecules around the methyl sites at 300 K.

	A1	τ_1	A2	τ_2	A3	τ_3	$\langle\tau\rangle$	R^2
CH3-1	0.259	0.127	0.454	2.459	0.287	7.488	3.297	0.9998
CH3-2	0.261	0.121	0.467	3.217	0.272	12.463	4.922	0.9997
CH3-3	0.258	0.116	0.437	3.332	0.305	14.133	5.800	0.9997
CH3-4	0.258	0.121	0.450	3.394	0.292	14.967	5.933	0.9997
CH3-5	0.259	0.120	0.444	3.287	0.297	12.981	5.347	0.9997
CH3-6	0.259	0.119	0.450	3.562	0.291	17.150	6.626	0.9997
CH3-7	0.260	0.116	0.439	3.697	0.301	18.209	7.135	0.9996
CH3-8	0.251	0.116	0.397	3.945	0.352	23.915	10.012	0.9996
CH3-9	0.260	0.122	0.460	3.868	0.279	20.447	7.526	0.9996
CH3-10	0.250	0.116	0.410	4.050	0.340	26.786	10.800	0.9996
CH3-11	0.253	0.118	0.418	3.915	0.329	24.150	9.600	0.9996
CH3-12	0.259	0.121	0.452	3.263	0.289	12.234	5.044	0.9997
CH3-13	0.258	0.121	0.466	3.779	0.276	20.302	7.393	0.9996
CH3-14	0.260	0.119	0.456	3.901	0.284	21.837	8.014	0.9996
CH3-15	0.253	0.118	0.427	3.862	0.320	20.755	8.316	0.9996
CH3-16	0.240	0.116	0.417	3.330	0.343	13.191	5.939	0.9998

Table S4 Tri-exponential fitting parameters and the integrated time (ps) of the SPC second rank rotation of hydration layer water molecules around the hydroxyl sites at 300 K.

	A1	τ_1	A2	τ_2	A3	τ_3	$\langle\tau\rangle$	R^2
OH-1	0.262	0.111	0.407	3.186	0.331	14.631	6.164	0.9997
OH-2	0.262	0.100	0.385	2.221	0.353	7.092	3.385	0.9998
OH-3	0.272	0.111	0.454	3.015	0.274	12.682	4.878	0.9996
OH-4	0.272	0.112	0.464	3.033	0.264	13.152	4.907	0.9996
OH-5	0.255	0.105	0.358	3.810	0.387	23.717	10.571	0.9996
OH-6	0.268	0.108	0.426	3.218	0.305	14.436	5.810	0.9996
OH-7	0.253	0.111	0.366	3.994	0.381	29.529	12.740	0.9996
OH-8	0.273	0.113	0.461	3.031	0.266	11.964	4.606	0.9996
OH-9	0.271	0.111	0.435	3.219	0.294	15.908	6.103	0.9996
OH-10	0.266	0.110	0.422	3.347	0.312	18.405	7.179	0.9996
OH-11	0.242	0.096	0.305	3.993	0.454	35.506	17.343	0.9995
OH-12	0.268	0.108	0.408	3.096	0.324	14.061	5.846	0.9997
OH-13	0.263	0.112	0.398	3.490	0.339	19.992	8.196	0.9996
OH-14	0.270	0.107	0.438	2.663	0.292	9.702	4.032	0.9997
OH-15	0.271	0.111	0.454	3.213	0.275	15.789	5.825	0.9996
OH-16	0.264	0.110	0.405	3.678	0.331	27.891	10.759	0.9995
OH-17	0.246	0.099	0.314	4.091	0.440	35.416	16.894	0.9995
OH-18	0.268	0.108	0.414	3.380	0.319	15.449	6.352	0.9996
OH-19	0.265	0.111	0.397	3.210	0.338	15.362	6.492	0.9996
OH-20	0.270	0.106	0.436	2.597	0.293	8.803	3.745	0.9997

OH-21	0.271	0.110	0.449	3.067	0.281	13.565	5.211	0.9996
OH-22	0.270	0.113	0.414	3.667	0.316	24.240	9.216	0.9995
OH-23	0.254	0.102	0.361	3.164	0.385	16.222	7.408	0.9997
OH-24	0.272	0.110	0.440	3.132	0.289	14.195	5.503	0.9996

REFERENCES

1. F. Sterpone, G. Stirnemann and D. Laage, *J. Am. Chem. Soc.*, 2012, **134**, 4116-4119.
2. A. C. Fogarty and D. Laage, *J. Phys. Chem. B*, 2014, **118**, 7715-7729.